fractal and fractional

MDPI

Article

Uncertainty Observer-Based Control for a Class of Fractional-Order Non-Linear Systems with Non-Linear Control Inputs

Juan Javier Montesinos-García [1], Jorge Luis Barahona-Avalos [1,*], Jesús Linares-Flores [1] and José Antonio Juárez-Abad [1]

Instituto de Electrónica y Mecatrónica, Universidad Tecnólogica de la Mixteca, Km 2.5 Carretera a Acatlima, Huajuapan de León, Oaxaca 69000, Mexico; jmontesinos@mixteco.utm.mx (J.J.M.-G.); jlinares@mixteco.utm.mx (J.L.-F.); abad@mixteco.utm.mx (J.A.J.-A.)
* Correspondence: jbarahona@mixteco.utm.mx

Abstract: This paper presents a novel control strategy based on an uncertainty estimator for a class of fractional-order nonlinear systems characterized by a polynomial input. The proposed strategy allows the system to be controlled without resorting to transformations or approximate linearization. This is accomplished by using a fractional-order sliding-mode observer, whose task is to estimate certain portions of the state of the nonlinear system of a non-integer order, thus allowing the control law to counteract these elements to steer the system towards a desired behavior. To validate the performance of the proposed strategy, it was implemented, both in simulation and experimentally, to regulate the temperature of the cold side of a thermoelectric module fed by a DC/DC electronic power converter of the step-down type, a system that is known to have a nonlinear polynomial-type control input.

Keywords: fractional-order; observer-based control; thermoelectric module

Citation: Montesinos-García, J.J.; Barahona-Avalos, J.L.; Linares-Flores, J.; Juárez-Abad, J.A. Uncertainty Observer-Based Control for a Class of Fractional-Order Non-Linear Systems with Non-Linear Control Inputs. *Fractal Fract.* **2023**, *7*, 836. https://doi.org/10.3390/fractalfract7120836

Academic Editors: Cristina I. Muresan, Aldo Jonathan Muñoz-Vazquez, Guillermo Fernández-Anaya and Oscar Martínez-Fuentes

Received: 30 September 2023
Revised: 27 October 2023
Accepted: 21 November 2023
Published: 25 November 2023

1. Introduction

Dynamical systems are commonly modeled using differential equations, which describe the system's behavior in terms of its states and their respective time derivatives. These derivatives are typically of an integer order; for example, the first derivative is of order 1, the second derivative is of order 2, and so forth.

An extension of the concept of derivatives and integrals allows for the consideration of orders that are not necessarily integer values. This extension involves fractional-order derivatives and integrals, which are studied within the field of fractional calculus. These extensions are known as fractional-order derivatives and integrals. When applied to the modeling of dynamical systems, they enhance the precision of the model by offering the flexibility to adjust the derivative order freely.

Fractional calculus has attracted interest due to the numerous potential applications in many disciplines such as finance [1], physics [2], medicine [3], biology [4], and control [5]. By applying fractional derivatives to known models and control laws, the model can better match the real-world dynamics of the system, whereas the fractional-order controller can find added benefits, similar to the Fractional Order Proportional Integral Derivative control (FOPID), which obtains two new values that can be adjusted for a better system response [6].

There have been recent advances on the control for fractional-order non-linear systems with non-linear control inputs: in [7], a sliding-mode control scheme with a fractional-order sliding surface is presented; in [8], a neural network controller for a fractional-order system with a non-linear control input is given, and in [9], a fractional-order control system is employed for a non-linear control input.

Fractional-order control applied to temperature regulation via thermoelectric modules (TEM) remains an area with limited exploration. In [10], a heating process is characterized by a fractional-order transfer function and subsequently regulated employing a fractional-order PID (FOPID) controller. Ref. [11] introduces an auto-tuning algorithm for FOPID controllers, based on particle swarm optimization techniques, and its performance is demonstrated through testing on a thermoelectric module. In a similar vein, ref. [12] tests the performance of a FOPID controller on a thermoelectric module, taking into consideration the process time delay. Meanwhile, ref. [13] advances the field by modeling an array of Peltier cells as a group of fractional-order transfer functions, where control is achieved using a set of PI controllers. Ref. [14] offers a similar approach, presenting a thermoelectric module modeled with an integer-order transfer function of the first order with a time delay and demonstrates a successful control implementation via the discrete approximation of a FOPID controller.

In addition to temperature regulation, thermoelectric modules find extensive application as thermoelectric generators. In this context, control is not directly applied on the thermoelectric module itself, but rather on the DC-DC power converter responsible for supplying energy to an energy storage device. The purpose of the controller is the optimization of the energy extraction process, a popular approach concerning the utilization of a Maximum Power Point Tracking (MPPT). Notably, a number of studies have explored the use of fractional-order controllers within the MPPT, with noteworthy contributions from works such as those presented in [15–18].

Thermoelectric modules have the capability of both heating and cooling, depending on the supplied current. This characteristic lends itself to various industrial applications, including thermal cycling in biomedical settings. In optics-based telecommunications, thermoelectric modules are employed for the cooling of lasers and other optical elements. Additionally, in spectroscopy, thermoelectric modules play a crucial role in the temperature regulation of deep-cooling CCD cameras. Thermoelectric generation stands as another important application of these modules. Moreover, certain consumer electronics rely on thermoelectric modules for cooling; for example, there exists a wide range of solutions based on these modules for cooling computer processors and graphics cards.

Given this diverse array of applications, the control of thermoelectric modules holds significant importance in engineering applications. Fractional-order models offer a superior adjustment for representing the dynamic behavior of real-world thermoelectric modules, allowing for the design of controllers with a more comprehensive understanding of the system and, consequently, yielding improved results. Despite the wide range of applications, there is a shortage of existing literature providing control methodologies beyond FOPID for fractional-order models of thermoelectric modules. This paper introduces a novel observer-based control strategy for commensurate fractional-order non-linear systems featuring non-linear polynomial control inputs. The proposed control law uses a state observer to mitigate the influence of the non-linear control inputs, thus inducing the desired response in the output of the TEM. By doing so, this new approach addresses a gap in current research and showcases its potential for enhancing the control performance of the fractional-order TEM model.

The rest of the paper is organized as follows: In Section 2, preliminaries about fractional calculus are given; Section 3 presents the observer-based control law; Section 4 is about the thermoelectric module; Section 5 contains numerical simulations; and Section 5 gives some concluding remarks.

2. Main Result

Preliminaries

The following definitions and lemmas constitute the mathematical basis of this work, as they allow us to establish the formal theoretical support of our proposal.

Definition 1. *The Caputo fractional derivative of order α of a function $f(t)$ is*

$$ {}_0^C D_t^\alpha f(t) = \frac{1}{\Gamma(n-\alpha)} \int_0^t f^{(n)}(\tau)(t-\tau)^{n-\alpha-1} d\tau \quad (1) $$

where $f^{(n)}(\tau)$ is the n-th order derivative and n is a positive integer number. $\Gamma(\cdot)$ is Euler's gamma function given by

$$ \Gamma(\alpha) = \int_0^\infty t^{\alpha-1} e^{-t} dt. \quad (2) $$

Definition 2. *The Riemann–Liouville fractional integral of a function $f(t)$ is*

$$ {}_0 I_t^\alpha f(t) = \frac{1}{\Gamma(\alpha)} \int_0^t f(\tau)(t-\tau)^{\alpha-1} d\tau \quad (3) $$

with $n-1 < \alpha < n$. This function converges to the right half of the complex plane.

Lemma 1 ([19]). *If a system has the equilibrium point $x = 0$, is contained within the domain $\mathbb{D} \subset \mathbb{R}$, and there is a continuously differentiable function such that $V[t, x(t)] : [0, \infty) \times \mathbb{D} \to \mathbb{R}$, the following conditions hold*

$$ \alpha_1 \|x\|^a \leq V[t, x(t)] \leq \alpha_2 \|x\|^{ab} \quad (4) $$

$$ {}_0^C D_t^\beta V[t, x(t)] \leq -\alpha_3 \|x\|^{ab} $$

with real numbers $\alpha_1, \alpha_2, \alpha_3, \beta, a, b > 0$, $t \geq 0$, $x \in \mathbb{D}$ and the order of the fractional derivative $0 \leq \beta \leq 1$, the equilibrium point $x = 0$ is said to be stable in the Mittag-Leffler sense, and therefore, asymptotically stable.

Lemma 2 ([20]). *The vector of differential functions $x(t) \in \mathbb{R}^n$ for a given time $t \geq 0$ fulfills*

$$ {}_0^C D_t^\alpha \left(x^T(t) P x(t) \right) \leq 2 x^T(t) P {}_0^C D_t^\alpha x(t) \quad (5) $$

with the constant, positive definite and the symmetric matrix $P \in \mathbb{R}^{n \times n}$.

3. Uncertainty Estimation Observer and Controller

The proposed control law employs a sliding-mode uncertainty observer to estimate the desired part of the system dynamics. This estimate is then employed via a sliding-mode controller to counteract the effects of the non-linear control input and to provide robustness to the closed-loop system.

Consider the fractional-order non-linear system with polynomial non-affine control inputs

$$ {}_0^C D_t^\alpha x = f(x) + \sum_{i=2}^{I} g(x) u^i + Bu \quad (6) $$

with $x, u \in \mathbb{R}^n$. The system can be separated in its power stage given by $x_l \in \mathbb{R}^m$, $m < n$:

$$ {}_0^C D_t^\alpha x_l = A_l x_l + B_l u + D_l(x) \quad (7) $$

having $x_l \in \mathbb{R}^m$, $m < n$ and the process with states containing the non-linear polynomial control inputs:

$$ {}_0^C D_t^\alpha x_{nl} = f_{nl}(x) + \sum_{i=2}^{I} g(x) x_{ul}^i + B_{nl} x_{ul} \quad (8) $$

where $x_{nl} \in \mathbb{R}^o$, $o < n$ and $x_{ul} \in x_l$, notice that the input of the non-linear function is one of the states of the power stage. The system can then be written as:

$$\begin{aligned} {}_0^C D_t^\alpha x_l &= A_l x_l + B_l u + D_l(x) \\ {}_0^C D_t^\alpha x_{nl} &= f_{nl}(x) + \sum_{n=2}^{N} g_n(x) x_{ul}^n + B_{nl} x_{ul} \\ y &= C_{nl} x_{nl} \end{aligned} \tag{9}$$

where A_l, B_l, C_{nl}, D_l and B_{nl} are matrices of the appropriate dimension, $x = (x_l, x_{nl})^T$, f_{nl} gives the non-linear dynamic of the system, and g_n are the coefficients of the non-linear polynomial control input. The output is the state to be controlled $y = C_{nl} x_{nl} = x_d$ with the fractional-order derivative

$${}_0^C D_t^\alpha x_d = f_d(x) + \sum_{n=2}^{N} g_{dn}(x) x_{ul}^n + B_{nld} x_{ul} \tag{10}$$

where $f_d(x)$, $g_{dn}(x)$, B_{nld} are the parts corresponding to the output of the system dynamics. The fractional-order derivative of x_d can be expressed as a two-state system by making the change in variable $x_d = \chi_1$

$$\begin{aligned} {}_0^C D_t^\alpha \chi_1 &= \chi_2 \\ {}_0^C D_t^\alpha \chi_2 &= {}_0^C D_t^\alpha C_{nl} x_d = f_d(x) + \sum_{n=2}^{N} g_{dn}(x) x_{ul}^n + B_{nld} x_{ul} \\ y_z &= \chi_1 \end{aligned} \tag{11}$$

In the interest of simplicity

$$f(\chi) = f_d(x) + \sum_{n=2}^{N} g_{dn}(x) x_{ul}^n + B_{nld} x_{ul} \tag{12}$$

then

$$\begin{aligned} {}_0^C D_t^\alpha \chi &= A\chi + f(\chi) D \\ y_\chi &= C\chi \end{aligned} \tag{13}$$

with $A = \begin{bmatrix} 0 & 1 \\ 0 & 0 \end{bmatrix}$, $D = \begin{bmatrix} 0 \\ 1 \end{bmatrix}$, $C = \begin{bmatrix} 1 & 0 \end{bmatrix}$. The following sliding-mode state observer produces an estimate of the fractional-order derivative of the state x_d:

$$\begin{aligned} {}_0^C D_t^\alpha \hat{\chi}_1 &= \hat{\chi}_2 + k_{l1}(\chi_1 - \hat{\chi}_1) + k_1 sign(\chi_1 - \hat{\chi}_1) \\ {}_0^C D_t^\alpha \hat{\chi}_2 &= k_{l2}(\chi_1 - \hat{\chi}_1) + k_2 sign(\chi_1 - \hat{\chi}_1) \end{aligned} \tag{14}$$

The synchronization error and its derivative of order α are then:

$$\begin{aligned} e &= \begin{bmatrix} \chi_1 - \hat{\chi}_1 \\ \chi_2 - \hat{\chi}_2 \end{bmatrix} = \begin{bmatrix} e_1 \\ e_2 \end{bmatrix} \\ {}_0^C D_t^\alpha e &= \begin{bmatrix} e_2 \\ f(\chi) - k_{l2}(e_1) + k_2 sign(e_1) \end{bmatrix} \end{aligned} \tag{15}$$

The following assumptions are needed for the proof of convergence for the observer.

Assumption 1. *There is a solution $P = P^T > 0$ for a $Q = Q^T > 0$ to the linear matrix inequality*

$$(A - K_{L1} C)^T P + P(A - K_{L1} C) + Q \leq 0 \tag{16}$$

Assumption 2. *The unknown dynamic is Lipschitz with* $L_1 > 0$, $L_1 \in \mathbb{R}$

$$\|f(x_1) - f(x_2)\| \quad \leq \quad L_1\|x_1 - x_2\| \tag{17}$$

Assumption 3. *For a number* $\Lambda > 0$, $\Lambda \in \mathbb{R}$, *the norm of the solution of the Lyapunov equation fulfills the inequality*

$$\|x_1 - x_2\|\|P\|L_1 \quad \leq \quad \Lambda \tag{18}$$

Assumption 4. *There is a solution* $P_l = P_l^T > 0$ *with* $Q_l = Q_l^T > 0$ *to the Lyapunov equation*

$$A_l^T P_l + P_l^T A_l \quad = \quad -Q_l \tag{19}$$

Assumption 5. *The states of the linear driving system are bounded via a real non-negative number* $\delta > 0$

$$x_l^T P_l D_x \quad \leq \quad \delta\|x_l\| \tag{20}$$

The observer equation is rewritten to match (13)

$$\begin{array}{rcl} {}_0^C D_t^\alpha \hat{\chi} & = & A\hat{\chi} + K_L Ce + Ksign(Ce) \\ \hat{y}_\chi & = & C\hat{\chi} \end{array} \tag{21}$$

where $K_L = \begin{bmatrix} k_{l1} & k_{l2} \end{bmatrix}^T$ and $K = \begin{bmatrix} k_1 & k_2 \end{bmatrix}^T$. The error dynamic is

$$\begin{array}{rcl} {}_0^C D_t^\alpha e & = & A\chi + f(\chi) - A\hat{\chi} - K_L Ce - Ksign(Ce) \\ & = & A(\chi - \hat{\chi}) + f(\chi)D - K_L Ce - Ksign(Ce) \\ & = & Ae + f(\chi)D - K_L Ce - Ksign(Ce) \end{array} \tag{22}$$

Consider the Lyapunov candidate function

$$V_1 \quad = \quad e^T Pe \tag{23}$$

From Lemma 2 and based on the Caputo derivative, the αth order derivative of the Lyapunov candidate function has the upper bound

$${}_0^C D_t^\alpha V_1 \quad \leq \quad 2e^T P {}_0^C D_t^\alpha e \tag{24}$$

By substituting the error dynamic into the fractional-order derivative of the Lyapunov candidate function

$$\begin{array}{rcl} {}_0^C D_t^\alpha V_1 & \leq & 2[Ae + f(\chi)D - K_L Ce - Ksign(Ce)]^T Pe \\ & & +2e^T P[Ae + f(\chi)D - K_L Ce - Ksign(Ce)] \end{array} \tag{25}$$

The terms of the derivative are rearranged

$$\begin{array}{rcl} {}_0^C D_t^\alpha V_1 & \leq & 2e^T \left[\left(A^T - K_L C \right) P + P(A - K_L C) \right] e \\ & & +2e^T P[f(\chi)D - Ksign(Ce)] \end{array} \tag{26}$$

From Assumption 1

$${}_0^C D_t^\alpha V_1 \quad \leq \quad 2e^T P[f(\chi)D - Ksign(Ce)] - e^T Qe \tag{27}$$

Using the Rayleigh–Ritz inequality $\lambda_{min}(Q)\|e\|^2 \leq e^T Qe \leq \lambda_{max}(Q)\|e\|^2$, then

$$\begin{aligned} {}_0^C D_t^\alpha V_1 &\leq 2e^T P[f(\chi)D - Ksign(Ce)] - \lambda_{max}(Q)\|e\|^2 \\ &\leq 2e^T P[f(\chi)D - Ksign(Ce)] \end{aligned} \tag{28}$$

Assumption 2 leads to

$$\begin{aligned} {}_0^C D_t^\alpha V_1 &\leq 2e^T Pf(\chi)D - 2e^T PKsign(Ce) \\ &\leq 2\left\|e^T\right\|\|P\|L_1\|x - \hat{x}\|\|D\| - 2e^T PKsign(Ce) \end{aligned} \tag{29}$$

From Assumption 3

$$\begin{aligned} {}_0^C D_t^\alpha V_1 &\leq 2\Lambda\|e\| - 2e^T PKsign(Ce) \\ &\leq 2\Lambda\|e\| - 2e^T PK\frac{Ce}{\|Ce\|} \\ &\leq 2\Lambda\|e\| - 2e^T PKC\frac{e}{\|C\|\|e\|} \\ &\leq 2\Lambda\|e\| - \frac{2}{\sqrt{\lambda_{max}C^T C}}e^T PKC\frac{e}{\|e\|} \end{aligned} \tag{30}$$

Knowing that $\sqrt{\lambda_{max}C^T C} = 1$

$$\begin{aligned} {}_0^C D_t^\alpha V_1 &\leq 2\Lambda\|e\|_2 - 2\lambda_{max}(PKC)\frac{\|e\|^2}{\|e\|} \\ &\leq 2\Lambda\|e\|_2 - 2\lambda_{max}(PKC)\|e\| \\ &\leq 2[\Lambda - \lambda_{max}(PKC)]\|e\| \end{aligned} \tag{31}$$

To fulfill Lemma 1, K has to satisfy the inequality $\lambda_{max}(PKC) > \Lambda$, so ${}_0^C D_t^\alpha V_1 \leq 0$ and the observer error is Mittag-Leffler stable. In order to estimate the desired part of the system dynamic, the state of the observer is extended by the equation

$${}_0^C D_t^\alpha \hat{z}_3 = k_3 sign(r - \hat{z}_3) \tag{32}$$

With r being a trajectory with the bounded αth-order Caputo derivative $\left\|{}_0^C D_t^\alpha r\right\| \leq \phi$, $\phi > 0$. The tracking error and its αorder derivative are

$$e_t = r - \hat{z}_3 \tag{33}$$

$${}_0^C D_t^\alpha e_t = {}_0^C D_t^\alpha (r - \hat{z}_3) \tag{34}$$

Let a Lyapunov candidate function for the error be

$$V_2 = e_t^T e_t \geq 0 \tag{35}$$

From Lemma 2, the αth-order derivative is bounded

$$\begin{aligned} {}_0^C D_t^\alpha V_2 &\leq 2e_t {}_0^C D_t^\alpha e_t \\ &\leq 2e_t\left({}_0^C D_t^\alpha e_t - {}_0^C D_t^\alpha \hat{z}_3\right) \\ &\leq 2e_t\left[{}_0^C D_t^\alpha r - k_3 sign(r - \hat{z}_3)\right] \\ &\leq 2e_t {}_0^C D_t^\alpha r - 2e_t k_3 sign(e_t) \end{aligned} \tag{36}$$

Since the derivative of the reference is bounded

$$\begin{aligned} {}_0^C D_t^\alpha V_2 &\leq 2\Phi e_t - 2e_t k_3 sign(e_t) \\ &\leq 2\Phi e_t - 2e_t k_3 \frac{e_t}{\|e_t\|} \\ &\leq 2\Phi \|e_t\| - 2k_3 \frac{\|e_t\|^2}{\|e_t\|} \\ &\leq 2(\Phi - k_3)\|e_t\| \end{aligned} \tag{37}$$

having $k_3 > \Phi$ makes the derivative of the Lyapunov candidate function be ${}_0^C D_t^\alpha V_2 \leq 0$; therefore, the additional observer satisfies Lemma 1, and thus, the additional state converges to the desired reference r. Choosing $r = \hat{z}_2 - B_{nl} x_{ul}$ leads to

$$\lim_{t\to\infty} \hat{z}_2 - u - \hat{z}_3 = 0 \tag{38}$$

$$\begin{aligned} \lim_{t\to\infty} \hat{z}_2 &= f_d(x) + \sum_{n=2}^{N} g_{dn}(x) x_{ul}^n + B_{nld} x_{ul} \\ \lim_{t\to\infty} (\hat{z}_2 - u - \hat{z}_3) &= \lim_{t\to\infty} \left[f_d(x) + \sum_{n=2}^{N} g_{dn}(x) x_{ul}^n + B_{nld} x_{ul} - B_{nld} x_{ul} - \hat{z}_3 \right] \\ \lim_{t\to\infty} \left[\left(f_d(x) + \sum_{n=2}^{N} g_{dn}(x) x_{ul}^n \right) - \hat{z}_3 \right] &= 0 \end{aligned} \tag{39}$$

The value $\hat{z}_3$ converges to the uncertain part of the dynamic containing the state and the non-linear part of the input $f_d(x) + \sum_{n=2}^{N} g_{dn}(x) x_{ul}^n$; thus, the extended dynamic for the observer is ${}_0^C D_t^\alpha z_3 = k_3 sign(\hat{z}_2 - u - \hat{z}_3)$.

A strategy similar to active disturbance rejection is proposed by using $\hat{z}_3$ to mitigate the effects of the non-linear control input, of which the input for the non-lineal system is $x_{ul} = -z_3 + u_d$, where u_d denotes the desired system-output dynamics. These dynamic are necessary to counteract the effects of any possible estimation errors by introducing a robust control law.

In order to attain the desired trajectory for x_{ul}, the linear part of the system is then expressed as

$$\begin{aligned} {}_0^C D_t^\alpha x_l &= A_l x_l + D_l + B_l u \\ y_l &= C_l x \end{aligned} \tag{40}$$

Let a differentiable desired reference signal for the linear system r_l with the bounded derivative $\left\| x_l P_l {}_0^C D_t^\alpha r_l \right\| \leq R\|x_l\|$, $R \geq 0$ and its tracking error e_l, with the fractional-order derivative, be

$$\begin{aligned} e_l &= r_l - x_l \\ {}_0^C D_t^\alpha e_l &= {}_0^C D_t^\alpha r_l - (A_l x_l + D_l + B_l u) \end{aligned} \tag{41}$$

Choosing $u = K_s sign(C_l e_l)$ as both the control input and a Lyapunov candidate function for the linear system

$$V_3 = {e_l}^T P_l e_l \tag{42}$$

According to Lemma 1

$${}_0^C D_t^\alpha V_3 \leq 2 e_l^T P_l {}_0^C D_t^\alpha e_l \tag{43}$$

$$\begin{aligned} {}_0^C D_t^\alpha V_3 &\leq 2e_l^T P_l \left[{}_0^C D_t^\alpha r_l - (A_l e_l + D_l(x) + B_l u) \right] \\ &\leq 2e_l^T P_l \left[{}_0^C D_t^\alpha r_l - (A_l e_l + D_l(x) + B_l u) \right] \\ &\leq 2e_l^T P_l {}_0^C D_t^\alpha r_l - {e_l}^T \left(A_l^T P_l + P_l^T A_l \right) e_l - 2e_l^T P_l D_l(x) - 2e_l^T P_l B_l u \end{aligned} \tag{44}$$

from Assumption 4

$$\begin{aligned} {}_0^C D_t^\alpha V_3 &\leq 2e_l^T P_l {}_0^C D_t^\alpha r_l - {e_l}^T Q e_l - 2e_l^T P_l D_l(x) - 2e_l^T P_l B_l u \\ &\leq 2e_l^T P_l {}_0^C D_t^\alpha r_l - 2e_l^T P_l D_l(x) - 2e_l^T P_l B_l u \end{aligned} \tag{45}$$

by Assumption 5

$$\begin{aligned} {}_0^C D_t^\alpha V_3 &\leq 2{e_l}^T P_l \left[{}_0^C D_t^\alpha r_l + \delta - K_s sign(C_l e_l) \right] \\ &\leq 2\|e_l\|(R+\delta) - 2{e_l}^T P_l K_s \frac{e_l}{\|e_l\|} \\ &\leq 2\|e_l\|(R+\delta) - 2\lambda_{max}(P_l K_s C_l)\|e_l\| \\ &\leq 2[R + \delta - 2\lambda_{max}(P_l K_s C_l)]\|e_l\| \end{aligned} \tag{46}$$

making k_3 so that $\delta + R < \lambda_{max}(P_l K_s C_l)$ leads to ${}_0^C D_t^\alpha V_3 \leq 0$; therefore, the input state for the non-linear states converges to the desired control law $-\hat{z}_3 + u_d$, making the overall system Mittag-Leffler stable with $u = K_s sign(-z_3 + u_d - C_l x)$.

4. The Thermoelectric Module and Numerical Results

Thermoelectric Modules (TEM) are solid-state temperature control devices composed of n- and p-type semiconductors linked to ceramic plates. Depending on the direction of the current provided to the semi-conductor elements of the module, heat is transferred from one of its ceramic plates to the other. The TEM is a non-linear system with a non-linear control input. An equivalent circuit model of the TEM is introduced in [21,22], which is especially practical for this application. In [23], an integer-order mathematical model for the TEM is obtained from the results of Lineykin. If the TEM is powered via a DC/DC Buck converter, the equations describing the TEM's state trajectories driven by the buck converter are similar to those in (9). Then, a fractional-order mathematical model for this system is given by

$$\begin{aligned} {}_0^C D_t^\alpha i_L &= \frac{E_u - v_c}{L} \\ {}_0^C D_t^\alpha v_c &= \frac{i_L}{C} - \frac{v_c - \gamma_s(T_c - T_h)}{CR_m} - \frac{v_c}{CR} \\ C_C {}_0^C D_t^\alpha T_c &= \frac{T_{amb}}{k_c} + \frac{T_h - T_c}{\sigma} - \frac{T_c}{k_c} \\ &\quad + \frac{v_c^2}{2_{Rm}} + \frac{k_s \gamma_s T_c v_c}{R_m \sigma} - \frac{\gamma_s(k_s + \theta_m) T_h v_c}{R_m \sigma} \\ &\quad + \left(\frac{\gamma_s^2 \theta_m}{2R_m \sigma} \right) \left(T_h^2 - T_c^2 \right) \\ C_h {}_0^C D_t^\alpha T_h &= \frac{T_{amb}}{k_c} + \frac{T_h - T_c}{\sigma} - \frac{T_c}{k_c} \\ &\quad + \frac{v_c^2}{2_{Rm}} + \frac{k_s \gamma_s T_c v_c}{R_m \sigma} - \frac{\gamma_s(k_s + \theta_m) T_h v_c}{R_m \sigma} \\ &\quad + \left(\frac{\gamma_s^2 \theta_m}{2R_m \sigma} \right) \left(T_h^2 - T_c^2 \right) \end{aligned} \tag{47}$$

where the output voltage is v_c, the electrical resistance parameter is R, the input PWM signal is u, the current of the converter is i_L, and the capacitance and inductance are denoted by C and L, respectively. The temperature in the cold side is T_c and the temperature in the hot plate is T_h; $\gamma_s$is the Seebeck coefficient; K_m is the thermal conductivity; R_m is the electric resistance; and $\triangle T$ is the temperature difference between the hot and cold plates; C_h and C_c are the thermal capacitance for the hot and cold plate, respectively; k_s is the thermal paste's thermal resistance; and θ_m is the thermal resistance of the system.

The linear part of the system is formed by the first two states and the remaining two are the non-linear dynamics of the TEM. The non-linear polynomial input for the TEM is the output voltage v_c. This input forms a second-degree polynomial with coefficients dependent on the parameters of the Buck and TEM, but it also depends on the TEM state. The order of the derivative α is obtained via system identification: first, the system parameters are identified using an integer-order mathematical model, and then a second parametric identification is conducted to estimate the value of the fractional derivative. The control law is tested in a TEC-12706 thermoelectric module; to make parameter identification easier, Equation (9) is simplified via a change in the variable:

$$\begin{aligned}
{}_0^C D_t^\alpha x_1 &= A_1 u - A_2 x_2 \\
{}_0^C D_t^\alpha x_2 &= B_1 x_1 - B_2 x_2 + B_3(x_3 - x_4) - B_4 x_2 \\
{}_0^C D_t^\alpha x_3 &= C_1 + C_2(x_4 - x_3) - C_3 x_3 + C_4 x_2^2 \\
&\quad + C_5 x_2 x_3 - C_6 x_2 x_4 + C_7\left(x_4^2 - x_3^2\right) \\
{}_0^C D_t^\alpha x_4 &= D_1 + D_2(x_3 - x_4) - D_3 x_4 + D_4 x_2^2 \\
&\quad + D_5 x_2 x_3 - D_6 x_2 x_4 + D_7\left(x_3^2 - x_4^2\right) \\
y &= x_3 = x_d
\end{aligned} \tag{48}$$

The parameter identification process yields the following results (Table 1):

Table 1. System parameters

New Variable	Numerical Value	New Variable	Numerical Value
A_1	0.002733	C_6	0.00227
A_2	0.000564	C_7	3.2930×10^{-8}
B_1	41.389	D_1	109.8051
B_2	41.38907	D_2	0.001649
B_3	1.3545	D_3	0.012514
B_4	0.003419	D_4	0.012039
C_1	243.79	D_5	0.00497
C_2	0.05489	D_6	0.00453
C_3	0.00392	D_7	5.82857
C_4	0.01242	α	0.912634
C_5	0.00314		

The observer-based proposed controller is then implemented using the CRONE approximation of the fractional-order integral

$$\begin{aligned} {}_0^C D_t^\alpha \hat{z}_1 &= \hat{z}_1 + k_{l1}(x_d - \hat{z}_1) + k_1 sign(x_d - \hat{z}_1) \\ {}_0^C D_t^\alpha \hat{z}_2 &= k_{l2}(x_d - \hat{z}_1) + k_2 sign(x_d - \hat{z}_1) \\ {}_0^C D_t^\alpha \hat{z}_3 &= k_3 sign(r - \hat{z}_3) \\ r &= \hat{z}_2 - B_{nl} x_{ul} \\ u &= K_s sign(-z_3 + u_d - C_l x) \end{aligned} \tag{49}$$

the gains for the controller are $k_{l1} = 3$, $k_{l2} = 4$, $k_1 = 200$, $k_2 = 200$, $k_3 = 20$, $K_s = 0.0011$, and $u_d = -12sign(273 + T_{des} - x_3)$, with T_{des} being a desired temperature in °C. Figure 1 shows the time evolution of the temperature on the cold side of the TEM at the desired temperatures of 20 °C, 18°C, and 16°C. Figure 2 shows the error signals for these desired temperatures, Figure 3 shows the behavior of the perturbation estimation, and Figure 4 shows the perturbation estimation error.

As shown in the figures, the simulation results obtained for the performance of the proposed controller were satisfactory. It is necessary to clarify that care must be taken in the way in which the gains are chosen so that the linear system obtains achievable values. It is important to note that the observer is compatible with other control techniques, such as FOPID and its variants.

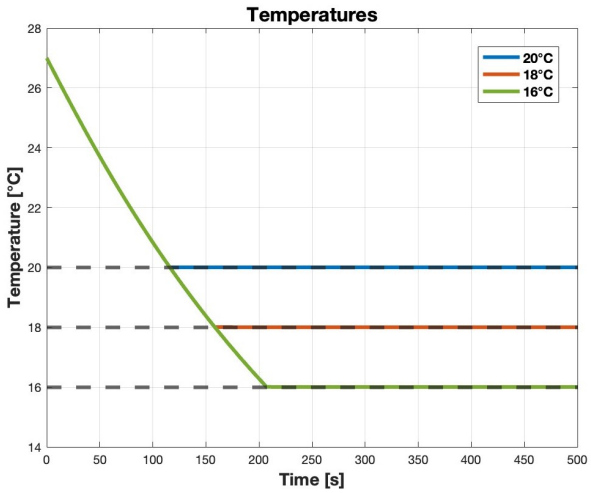

Figure 1. Temperature of the cold plate.

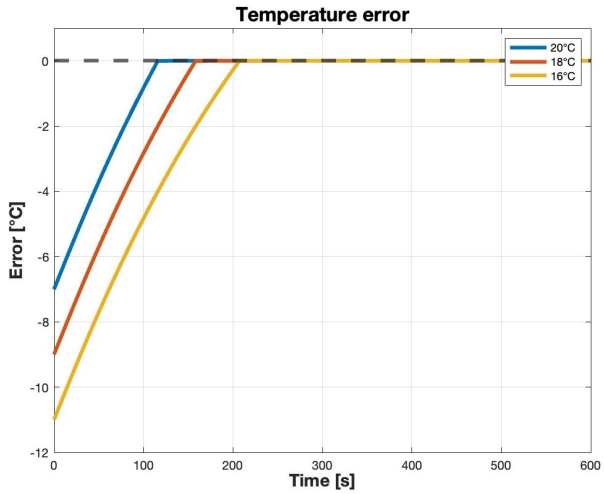

Figure 2. Temperature tracking error for the cold plate.

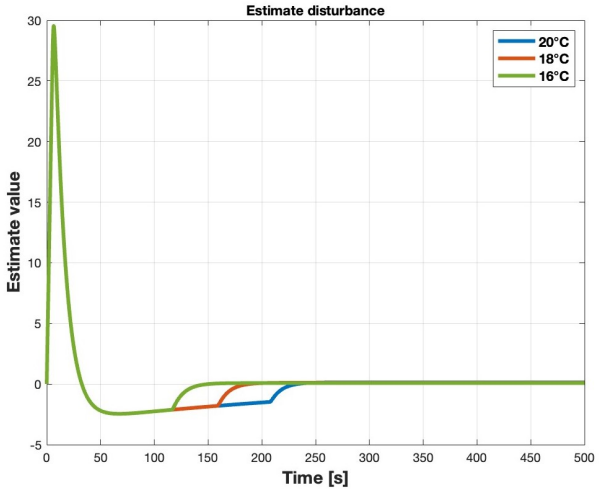

Figure 3. Estimated disturbance by the observer.

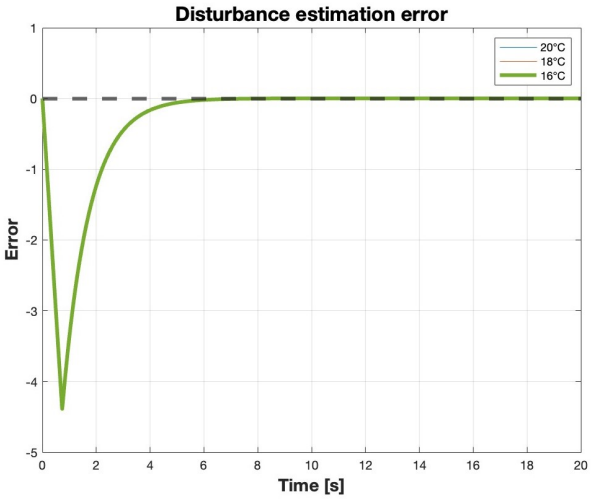

Figure 4. Disturbance estimation error.

Notice the observer consistently generates identical error trajectories across all experiments; as depicted in Figure 4, each trajectory is consistently replicated. To confirm the validity of the simulation, the experiments were conducted on an experimental platform. The control law is implemented using an Arduino board for control and data acquisition. The next figures (Figures 5–8) show the results of the experiment.

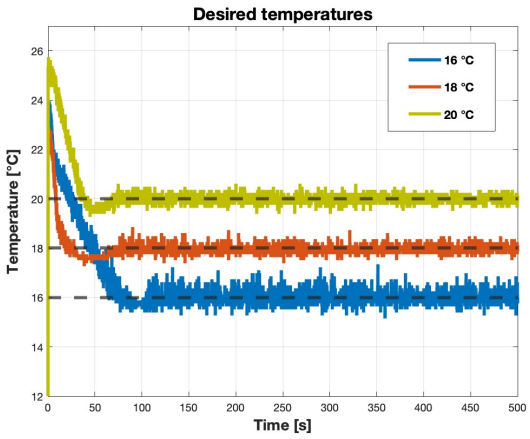

Figure 5. Measured temperature of the cold plate.

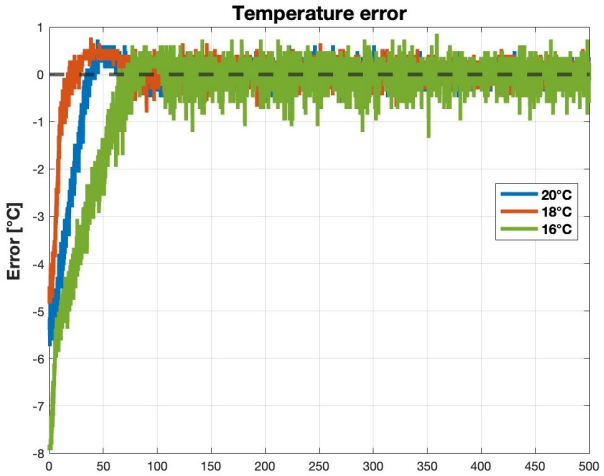

Figure 6. Measured temperature error.

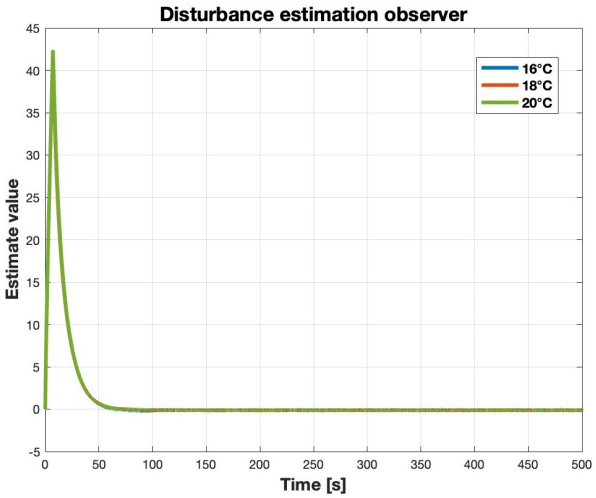

Figure 7. Estimated disturbance by the observer during experiment.

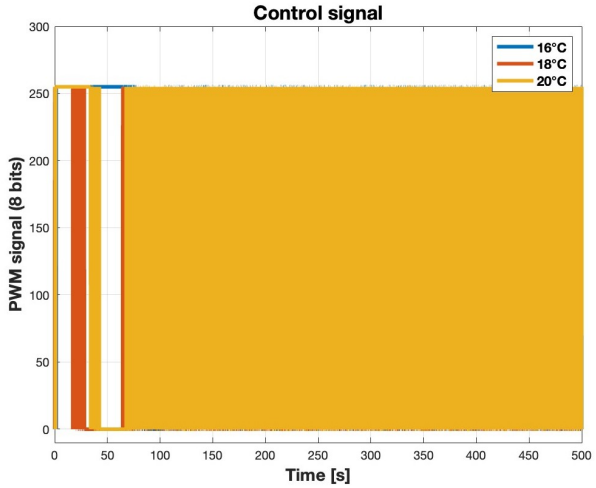

Figure 8. Control input.

The experiment shows that the control law is effective in a real-life scenario and behaves very similarly to the simulation results. It is worth mentioning that the initial conditions cannot be the same for each experiment because they were conducted at different times of the day or even on different days; thus, room temperature is different, making each

initial condition different. To make the experiment have the same initial condition each time would require equipment to accurately regulate room temperature, and the authors have no access to said equipment. Next, an experiment to test disturbance rejection is made in which a fan is used to raise the temperature of the TEM (Figure 9):

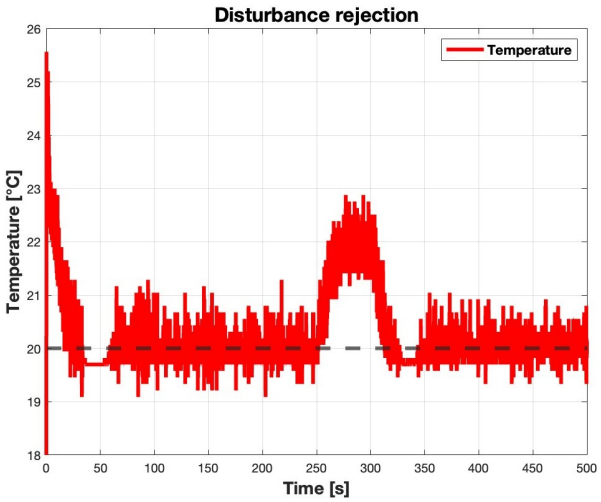

Figure 9. Disturbance rejection.

The controller effectively corrects the offset in temperature caused by the air stream, showing its capability to reject disturbances. Finally, it is compared to a FOPID controller similar to the one proposed on [24], of which the desired temperature is 20 °C (Figures 9 and 10):

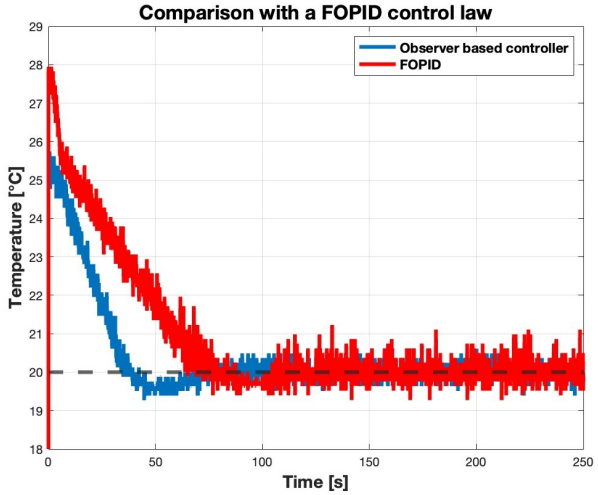

Figure 10. Comparison of the proposed observer-based controller to a PI controller.

The observer-based controller exhibits a notably shorter settling time when contrasted with the FOPID controller. Furthermore, the FOPID controller displays a minor steady-state error, caused by its tendency to overreact to the sluggish response of the thermal system when the temperature error becomes positive. Additionally, it is worth mentioning that the implementation of the FOPID controller poses an increased computational cost on the microcontroller. This arises from the distinct orders of the integral and derivative gains.

5. Conclusions

In this paper, a fractional-order, observer-based, sliding-mode control law is proposed to regulate a non-linear system with non-linear control inputs. The control law is validated

through testing on a Thermoelectric Module powered via a buck converter, a system known for its non-linear control inputs. The simulation results validate that the control law can guide the system to a desired value. The uncertainty observer achieves its purpose of making an estimate of the desired part of the state and, consequently, this estimate can be used to mitigate the effects of the non-linear control input and give the system output the desired dynamic. The simulation results are corroborated via implementation in an experimental platform, which gives similar results.

As highlighted in the introduction, there is a scarcity of research focusing on TEM control utilizing diverse fractional-order control laws. In future work, the authors intend to expand on the applications for the temperature-based control of the TEM by employing consensus control to synchronize an array of thermoelectric modules for cooling applications. In this setting, it is also desirable to introduce optimal control techniques for lowering the power consumption and make the cooling system more cost effective; as it is widely known, TEM are not efficient cooling devices. This next work also intends on applying other definitions of the fractional-order derivative, such as Caputo–Fabrizio and Atangana–Baleanu.

Author Contributions: Conceptualization, J.J.M.-G.; investigation, J.J.M.-G., J.L.B.-A., J.L.-F. and J.A.J.-A.; writing—original draft, J.J.M.-G. and J.L.B.-A.; writing—review and editing, J.L.B.-A.; supervision, J.L.B.-A. All authors have read and agreed to the published version of the manuscript.

Funding: This research received no external funding.

Data Availability Statement: No new data were created or analyzed in this study. Data sharing is not applicable to this article.

Conflicts of Interest: The authors declare no conflict of interest.

References

1. Laskin, N. Fractional market dynamics. *Phys. Stat. Mech. Appl.* **2000**, *287*, 482–492 [CrossRef]
2. Hilfer, R. (Ed.) *Applications of Fractional Calculus in Physics*; World Scientific: Singapore, 2000.
3. Zhou, X.J.; Gao, Q.; Abdullah, O.; Magin, R.L. Studies of anomalous diffusion in the human brain using fractional order calculus. *Magn. Reson. Med.* **2010**, *63*, 562–569. [CrossRef] [PubMed]
4. Freeborn, T.J. A survey of fractional-order circuit models for biology and biomedicine. *IEEE J. Emerg. Sel. Top. Circuits Syst.* **2013**, *3*, 416–424. [CrossRef]
5. Liu, H.; Li, S.; Li, G.; Wang, H. L1 Adaptive controller design for a class of uncertain fractional-order nonlinear systems: An adaptive fuzzy approach. *Int. J. Fuzzy Syst.* **2018**, *20*, 366–379. [CrossRef]
6. Podlubny, I.; Dorcak, L.; Kostial, I. On fractional derivatives, fractional-order dynamic system and PID-controllers. In Proceedings of the 36th 1997 IEEE Conference on Decision and Control, Phoenix, AZ, USA, 7–10 December 1999; pp. 4985–5990.
7. Dang, V.T.; Nguyen, D.B.H.; Tran, T.D.T.; Le, D.T.; Nguyen, T.L. Model-free hierarchical control with fractional-order sliding surface for multisection web machines. *Int. J. Adapt. Control. Signal Process.* **2023**, *37*, 497–518. [CrossRef]
8. Zouari, F.; Ibeas, A.; Boulkroune, A.; Jinde, C.A.O.; Arefi, M.M. Neural network controller design for fractional-order systems with input nonlinearities and asymmetric time-varying Pseudo-state constraints. *Chaos Solitons Fractals* **2021**, *144*, 110742. [CrossRef]
9. Hu, X.; Song, Q.; Ge, M.; Li, R. Fractional-order adaptive fault-tolerant control for a class of general nonlinear systems. *Nonlinear Dyn.* **2020**, *101*, 379–392. [CrossRef]
10. Macias, M.; Sierociuk, D. Fractional order calculus for modeling and fractional PID control of the heating process. In Proceedings of the 13th International Carpathian Control Conference (ICCC), High Tatras, Slovakia, 28–31 May 2012; pp. 452–457. [CrossRef]
11. Maamir, F.; Guiatni, M.; Hachemi, H.M.S.M.E.; Ali, D. Auto-tuning of fractional-order PI controller using particle swarm optimization for thermal device. In Proceedings of the 2015 4th International Conference on Electrical Engineering (ICEE), Boumerdes, Algeria, 13–15 December 2015; pp. 1–6. [CrossRef]
12. Kungwalrut, P.; Numsomran, A.; Chaiyasith, P.; Chaoraingern, J.; Tipsuwanporn, V. A PID controller design for peltier-thermoelectric cooling system. In Proceedings of the 2017 17th International Conference on Control, Automation and Systems (ICCAS), Jeju, Republic of Korea, 18–21 October 2017; pp. 766–770. [CrossRef]
13. Viola, J.; Rodriguez, C.; Chen, Y. PHELP: Pixel Heating Experiment Learning Platform for Education and Research on IAI-based Smart Control Engineering. In Proceedings of the 2020 2nd International Conference on Industrial Artificial Intelligence (IAI), Shenyang, China, 22–23 July 2020; pp. 1–6. [CrossRef]
14. Viola, J.; Oziablo, P.; Chen, Y. A Portable and Affordable Networked Temperature Distribution Control Platform for Education and Research. *IFAC-PapersOnLine* **2020**, **53**, 17530–17535. [CrossRef]

15. Olabi, A.G.; Rezk, H.; Sayed, E.T.; Awotwe, T.; Alshathri, S.I.; Abdelkareem, M.A. Optimal Parameter Identification of Single-Sensor Fractional Maximum Power Point Tracker for Thermoelectric Generator. *Sustainability* **2023**, *15*, 5054. [CrossRef]
16. Rezk, H.; Olabi, A.G.; Ghoniem, R.M.; Abdelkareem, M.A. Optimized Fractional Maximum Power Point Tracking Using Bald Eagle Search for Thermoelectric Generation System. *Energies* **2023**, *16*, 4064. [CrossRef]
17. Rezk, H.; Zaky, M.M.; Alhaider, M.; Tolba, M.A. Robust Fractional MPPT-Based Moth-Flame Optimization Algorithm for Thermoelectric Generation Applications. *Energies* **2022**, *15*, 8836. [CrossRef]
18. Abdullah, A.M.; Rezk, H.; Elbloye, A.; Hassan, M.K.; Mohamed, A.F. Grey Wolf Optimizer-Based Fractional MPPT for Thermoelectric Generator. *Intell. Autom. Soft Comput.* **2021**, *29*, 730–740. [CrossRef]
19. Li, Y.; Chen, Y.; Podlubny, I. Stability of fractional- order nonlinear dynamic systems: Lyapunov direct method and generalized Mittag-Leffler stability. *Comput. Math-Ematics Appl.* **2010**, *59*, 1810–1821. [CrossRef]
20. Duarte-Mermoud, M.A.; Aguila-Camacho, N.; Gallegos, J.A.; Castro-Linares, R. Using general quadratic Lyapunov functions to prove Lyapunov uniform stability for fractional order systems. *Commun. Nonlinear Sci. Numer. Simul.* **2015**, *22*, 650–659. [CrossRef]
21. Lineykin, S.; Ben-Yaakov, S. Analysis of thermoelectric coolers by a spice-compatible equivalent-circuit model. *IEEE Power Electron. Lett.* **2005**, *3*, 63–66. [CrossRef]
22. Lineykin, S.; Ben-Yaakov, S. Modeling and analysis of thermoelectric modules. *IEEE Trans. Ind. Appl.* **2007**, *43*, 505–512. [CrossRef]
23. Barahona-Avalos, J.L.; Juárez-Abad, J.A.; Galván-Cruz, G.S.; Linares-Flores, J. *Control Mediante Rechazo Activo de Perturbaciones de la Temperatura de un Módulo Termoeléctrico*; Revista Iberoamericana de Automática e Informática Industrial: Valencia, España, 2021.
24. Liu, L.; Xue, D.; Zhang, S. General type industrial temperature system control based on fuzzy fractional-order PID controller. *Complex Intell. Syst.* **2023**, *9*, 2585–2597. [CrossRef]